Proteomics Identification of Sorting Nexin 27 as a Diacylglycerol Kinase ζ-associated Protein

NEW DIACYLGLYCEROL KINASE ROLES IN ENDOCYTIC RECYCLING*

Esther Rincón‡§, Teresa Santos‡, Antonia Ávila-Flores¶‖, Juan P. Albar, Vasiliki Lalioti‡‡, Cai Lei§§, Wanjin Hong§§, and Isabel Mérida‡¶¶**

Diacylglycerol kinase ζ is a member of the diacylglycerol kinase family of enzymes, which generate phosphatidic acid through diacylglycerol phosphorylation. In addition to the catalytic and cysteine-rich domains found in all diacylglycerol kinases, diacylglycerol kinase ζ has a MARCKS domain as well as a C-terminal region containing four ankyrin repeats and a PDZ-binding motif. Previous reports demonstrated that diacylglycerol kinase ζ interaction with several proteins is an important mechanism for modulating the localization and activity of this enzyme. Here we used a proteomics approach to search for novel diacylglycerol kinase ζ-interacting proteins and identified sorting nexin 27 (SNX27), a recently described member of a protein family involved in intracellular trafficking, which has a PDZ domain in addition to the phox homology domain characteristic of SNX proteins. Co-immunoprecipitation studies and two-hybrid analysis confirmed physical, PDZ-dependent association between SNX27 and diacylglycerol kinase ζ. Because diacylglycerol kinase ζ is expressed abundantly in T lymphocytes, we characterized SNX27 expression and subcellular localization in these cells. SNX27 co-localized with transferrin receptor-positive vesicles, pointing to its participation in T cell endocytic recycling. Expression of deletion mutants revealed that in addition to the phox homology domain the SNX27 PDZ domain contributed to vesicle localization of this protein, suggesting that interaction with diacylglycerol kinase ζ regulates SNX27 localization. Analysis of cells with RNA interference-mediated knockdown of diacylglycerol kinase ζ showed accelerated transferrin receptor exit from the lymphocyte endocytic recycling compartment back to the plasma membrane, further confirming diacylglycerol kinase ζ-dependent control of vesicle trafficking. These data support a previously unreported role for diacylglycerol kinase ζ in the modulation of membrane trafficking, which may also help to define SNX27 function. ***Molecular & Cellular Proteomics 6:1073–1087, 2007.***

From the Departments of ‡Immunology and Oncology and **Proteomics, Centro Nacional de Biotecnología/CSIC, E-28049 Madrid, Spain, ¶Servicio de Inmunología, Hospital de la Princesa and ‡‡Centro de Biología Molecular Severo Ochoa/Consejo Superior de Investigaciones Científicas (CSIC), Universidad Autónoma de Madrid, E-28049, Spain, and §§Membrane and Biology Laboratory, Institute of Molecular and Cell Biology, 117609 Singapore, Singapore

Received, February 5, 2007, and in revised form, March 2, 2007

Published, MCP Papers in Press, March 9, 2007, DOI 10.1074/mcp.M700047-MCP200

Intracellular membrane traffic requires a complex molecular machinery with a plethora of small GTPases, adaptors, and coat components that must be assembled and disassembled in different steps to ensure correct vesicle formation. Membrane lipids are key components in this process; many proteins involved in vesicle formation have lipid-binding domains, and modulation of lipid-modifying enzymes profoundly alters secretion and/or endocytosis (1).

Diacylglycerol (DAG)[1] is a lipid with important functions in membrane trafficking. When generated in restricted membrane regions, the characteristic negative curvature of DAG promotes the membrane constriction essential for fission and the instability required for fusion (2–5). In addition to modifying membrane characteristics, DAG binds to and activates various proteins needed for vesicle formation, such as protein kinase D and ADP-ribosylation factor (Arf) GTPase-activating protein (6, 7). In addition to DAG, phosphatidic acid (PA) also confers the negative curvature that facilitates vesicle fission or fusion (3, 8–10). PA can also bind to and activate enzymes that participate in membrane trafficking, such as coatomer, Arf, *N*-ethylmaleimide-sensitive factor, kinesin, phosphatidylinositol-4-phosphate 5-kinase, and Arf6 GTPase-activating protein (11–15).

The diacylglycerol kinase (DGK) family is an evolutionarily conserved family of lipid kinases that phosphorylate DAG to produce PA (16). All members of the family have at least two N-terminal cysteine-rich domains (C1) and a conserved catalytic domain. These proteins have additional functional domains that allow their classification into five subgroups (I–V). Their structural diversity, distinct tissue expression, and specific intracellular localization confer on each DGK isoform the ability to regulate different DAG and PA pools and thus to participate in diverse signaling complexes (17).

[1] The abbreviations used are: DAG, diacylglycerol; Ab, antibody; Ank, ankyrin; BAR, Bin/amphiphysin/Rvs; CT, C-terminal; DGK, diacylglycerol kinase; EEA1, early endosomal antigen 1; ERC, endocytic recycling compartment; FL, full-length; X-α-gal, 5-bromo-4-chloro-3-indolyl-α-D-galactopyranoside; GFP, green fluorescent protein; HA, hemagglutinin; HEK, human embryonic kidney; HIV-1, human immunodeficiency virus, type 1; IF, immunofluorescence; IS, immunological synapse; PA, phosphatidic acid; PDZbm, PDZ-binding motif; PI, phosphatidylinositol; PI3K, phosphoinositide-3-OH kinase; PKC, protein kinase C; PX, Phox homology; PDZ, postsynaptic density protein, disc-large, and zonula occludens-1; PLD, phospholipase D; RA, Ras association; RNAi, RNA interference; SNX, sorting nexin; TCR, T cell receptor; TfR, transferrin receptor; Tf-Rhod, transferrin tetramethylrhodamine; WB, Western blot; SD, synthetic dropout.

DGKζ belongs to the type IV DGK family, characterized by a MARCKS (myristoylated alanine-rich protein kinase C (PKC) kinase substrate) homology domain as well as a C-terminal region with four ankyrin (Ank) repeats and an ETAV sequence (18). These four amino acids can bind the class I PDZ (postsynaptic density protein, disc-large, and zonula occludens-1) domain, thus constituting a PDZ-binding motif (PDZbm) (19). DGKζ is expressed ubiquitously and is associated with cell cycle regulation, cytoskeletal reorganization, and modulation of the immune response among other functions (20–24).

DGKζ is expressed abundantly in T lymphocytes; studies using GFP-coupled DGKζ chimeras in live T cells demonstrated receptor-dependent membrane translocation of this enzyme (25).This analysis indicated that the C-terminal region of the protein confers specificity for protein translocation, suggesting the importance of regulation based on protein-protein interactions. Accordingly recent studies showed DGKζ interaction with several proteins such as PKC, Rac, syntrophins, leptin receptor, and Src (23, 26–29), indicating that DGKζ functions may be largely dependent on the formation of distinct protein complexes.

Using a mass spectrometry-based analysis of DGKζ-interacting proteins, we identified sorting nexin 27 (SNX27), a member of the SNX family of proteins involved in membrane traffic and protein sorting (30, 31). The association between these proteins was direct and was mediated by interaction of the SNX27 PDZ domain with the C terminus of DGKζ. SNX27 was expressed in hematopoietic cells and localized to the endocytic recycling system of T lymphocytes. Finally we traced transferrin receptor (TfR) recycling, which was accelerated in cells with diminished DGKζ levels. Our results identify SNX27 as a new DGKζ-binding protein and unveil a function for SNX27·DGKζ complex in the control of protein trafficking of T cells.

EXPERIMENTAL PROCEDURES

Reagents and Antibodies—Orthovanadate, PMSF, poly(DL-lysine) and Igepal CA-630 were from Sigma. Leupeptin and aprotinin were purchased from Roche Applied Science, wortmannin was from Calbiochem, and transferrin tetramethylrhodamine (Tf-Rhod) was from Molecular Probes (Leiden, The Netherlands). Rabbit polyclonal anti-DGKζ antibody (Ab) raised against a C-terminal peptide was a generous gift of Dr. Kaoru Goto (Department of Anatomy and Cell Biology, Yamagata University School of Medicine, Yamagata, Japan) (32). Rabbit polyclonal anti-DGKζ Ab raised against an N-terminal peptide was a generous gift of Dr. M. K. Topham (University of Utah, Salt Lake City, UT) (33). To generate the polyclonal anti-SNX27, the N-terminal 265-residue fragment of SNX27, which contains PDZ and phox homology (PX) domains, was produced as a GST fusion protein in bacteria. The fragment was cleaved with thrombin and used to immunize rabbits with Freund's adjuvant (Invitrogen). To affinity purify antibodies to SNX27, serum from immunized rabbits was incubated with the antigen coupled to cyanogen bromide-activated Sepharose (Amersham Biosciences). Bound antibody was eluted with Immuno-Pure IgG elution buffer (Pierce), neutralized with PBS, pH 7.4, and then dialyzed against the same solution. We used the following mouse monoclonal antibodies: anti-hemagglutinin (anti-HA) (Babco, Richmond, CA), -Myc (Cell Signaling Technology, Danvers, MA), -GST (Santa Cruz Biotechnology, Santa Cruz, CA), -GFP (Roche Applied Science), -tubulin (Sigma), -early endosomal antigen 1 (EEA1), -GM130 and -SNX2 (BD Transduction Laboratories), and -CD63 (Oncogene Research, San Diego, CA). Mouse anti-human TfR and rabbit anti-Rab11 were from Zymed Laboratories Inc.. The monoclonal Ab to human LAMP1 developed by J. Thomas August and James E. K. Hildreth was obtained from the Developmental Studies Hybridoma Bank (developed under the auspices of the NICHD, National Institutes of Health and maintained by the Department of Biological Sciences, University of Iowa, Iowa City, IA). Cy3- and Cy5-conjugated antibodies were from Jackson ImmunoResearch Laboratories (West Grove, PA), and Alexa 488-conjugated Ab was from Molecular Probes.

Plasmids and DNA Constructs—The pcDNA3MycDGKζ, GFP-DGKζ, and HA-DGKζCT constructs were described previously (25). For generation of GST fusion proteins, pcDNA3MycDGKζ was BglII-digested, blunted, and KpnI-digested, and the 3.9-kb fragment was subcloned in the pEBG eukaryotic GST vector digested with KpnI/ClaI (GST-DGKζFL). The construct encoding the C-terminal region of the protein (GST-DGKζCT, including the four ankyrin repeats and the PDZbm) was excised from pGEM-T with NotI and then subcloned in pEBG vector digested with NotI. The human Myc-tagged SNX27*b* full length (Myc-SNX27*b*FL) was described previously (34). Myc-tagged deletion mutants (Myc-SNX27*b*ΔRA/-SNX27*b*ΔPX/-SNX27*b*RA) were generated from the full-length SNX27*b* using PCR and subcloned into pDMyc-neo vector, which is a modified version of the pCIneo vector (Stratagene) (35), with the same restriction enzyme sites as above. All constructs were confirmed by sequencing. The coding region corresponding to mouse SNX27*a* cloned into the pSPORT1 vector was obtained from Open Biosystems (Clone number 6431126, GenBank™ accession number BC053495); pSPORT1-SNX27*a* was digested with SalI/BamHI, and the 1.7-kb fragment was subcloned in pEGFP-C2 digested with SalI/BamHI. To generate GFP-SNX27*a*ΔPDZ, the sequence ^{336}TCCGAG^{341} in GFP-SNX27*a* was mutated to GTCGAC to generate a SalI site. Site-directed mutagenesis was performed using the QuikChange mutagenesis kit (Stratagene). The plasmid was cleaved with SalI, and the resulting 6.4-kbp fragment lacking the PDZ domain was then religated.

For yeast two-hybrid interaction assays, four DGKζ constructs were subcloned in pGBKT7 vector fused to GAL4BD as bait, the SNX27 N-terminal region (containing the PDZ and PX domains) was subcloned into pGADT7 vector fused to GAL4AD, and pGBKT7DGKζFL was generated by digesting pcDNA3MycDGKζ with EcoRI, and the 3.4-kb fragment was subcloned into EcoRI-digested pGBKT7. pGBKT7DGKζΔAnk was generated from pGBKT7DGKζFL digested with SacI and religated. To generate pGBKT7DGKζΔPDZbm, GFP-DGKζΔPDZbm was digested with NcoI, blunted, and digested with EcoRI/AflII; the 2.9-kb fragment was subcloned in pGBKT7 digested with EcoRI/SmaI. The pGBKT7CT construct, including the four ankyrin repeats and PDZbm, was generated by PCR from GFP-DGKζFL with appropriate primers (AnkPDZ1, 5′-GAATTCGCACTGCCCCAAGGTGAAG-3′; AnkPDZ, 5′-GTCGACTACACAGCTGTCTCCTGGTCC-3′), including two restriction sites, EcoRI and SalI. The 430-bp PCR product was subcloned in the pGEM-T Easy vector and then excised with EcoRI/SalI for subcloning in EcoRI/SalI-digested pGBKT7. To generate pGADT7SNX27ΔRA, pCIneoSNX27 was digested with XhoI/XbaI, and the 730-bp fragment containing the N-terminal portion of the protein was subcloned in pCDNA3 digested with XhoI/XbaI (pCDNA3SNX27ΔRA). pCDNA3SNX27ΔRA was digested with XbaI, blunted, and EcoRI-digested; the 730-bp fragment was subcloned in pGADT7 digested with EcoRI/SmaI.

Cell Lines and Transient Transfection—The rat basophilic leukemia mast cell line was provided by Dr. S. Corbalán García (Departamento de Bioquímica y Biología Molecular, Universidad de Murcia, Murcia, Spain). The following cell lines were obtained from the American Type Culture Collection (ATCC, Manassas, VA): K562 human chronic myelogenous leukemia, the CTLL2 mouse cytotoxic cell line, the EL4 mouse T lymphoma, Jurkat human acute T cell leukemia, and

HEK293/HEK293T human embryonic cell lines. Thymocytes were obtained from BALB/c mice following standard protocols, and dendritic cells were from Dr. C. F. Ardavín (Centro Nacional de Biotecnología/CSIC, Madrid, Spain). Jurkat, HEK293, and HEK293T cell lines were cultured in Dulbecco's modified Eagle's medium (BioWhittaker, Walkersville, MD) supplemented with 10% FCS (Sigma) and 2 mM glutamine (37 °C, 5% CO_2). Jurkat cells in logarithmic growth phase were transfected (1.2×10^7 in 400 ml of complete medium) with 20 μg of plasmid DNA by electroporation with a Gene Pulser (Bio-Rad; 270 V, 975 microfarads); cells were immediately transferred to 10 ml of complete medium and assayed after 24 h. HEK293T and HEK293 cells were transfected using Jet-PEI reagent (PolyPlus Transfection, Illkirch, France) and Lipofectamine Plus (Invitrogen), respectively.

Purification of DGKζ-associated Proteins—For transfection, HEK293T cells were plated in 150-mm culture dishes. When cells reached 60% confluence (24 h), GST, GST-DGKζFL, and GST-DGKζCT transfection was carried out using Jet-PEI. After 24 h, cells were lysed in Nonidet P-40 buffer (150 mM NaCl, 10 mM NaF, 10 mM $Na_4P_2O_7$, 50 mM Tris-HCl, pH 7.5, 1% Igepal CA-630, and 0.5 mM PMSF/protease inhibitor mixture), and lysates were centrifuged (20,800 × *g*, 10 min, 4 °C). Supernatants were incubated with glutathione-Sepharose 4B (Amersham Biosciences) (overnight, 4 °C) to batch purify GST recombinant proteins. Beads were then washed extensively with BC500 buffer (25 mM Tris-HCl, pH 7.8, 500 mM NaCl, 1 mM EDTA, 1 mM dithiothreitol, 10% glycerol, 0.2% Igepal CA-630, 1% Triton X-100, and 0.1% sodium deoxycholate). Finally bound proteins were eluted with 5× Laemmli buffer (36). Aliquots of eluted proteins were analyzed by 7.5% SDS-PAGE and visualized by Coomassie Blue staining. Bands of interest were excised and analyzed by MS.

Coomassie Blue-stained bands were excised manually from gels, deposited in 96-well plates, and processed automatically in an Investigator ProGest protein digestion station (Genomics Solutions, Cambridgeshire, UK) where samples were in-gel-reduced, alkylated with iodoacetamide, and trypsin-digested (37). Resulting peptides were analyzed by MALDI-TOF MS; 0.3 μl of matrix solution (5 mg/ml 2,5-dihydrobenzoic acid in 33% (v/v) aqueous acetonitrile and 0.1% (v/v) trifluoroacetic acid) was added to an AnchorChip MALDI target (Bruker Daltonics GmbH, Bremen, Germany) and allowed to dry at room temperature. A 0.3-μl aliquot of each peptide mixture was then deposited onto matrix surfaces and dried at room temperature.

MALDI mass spectra were acquired automatically on a Bruker Reflex IV MALDI-TOF mass spectrometer (Bruker Daltonics) by FlexControl 1.1 software and processed by Xtof 5.1.1 software to analyze raw data. Each spectrum was calibrated internally with two trypsin autolysis reference ions, specifically 842.510- and 2211.105-Da peptides, to reach a typical mass measurement accuracy of ±30 ppm in the 800–3000 *m/z* range. All known contaminants were excluded during the process. The parameters used to analyze data were a signal-to-noise threshold of 20 and resolution higher than 4000.

Database Search—For protein identification, tryptic peptide masses were transferred to the BioTools 2.0 interface (Bruker Daltonics) to search in the National Center for Biotechnology non-redundant (NCBInr) database using Mascot software (Matrix Science, London, UK). Search parameters were set as follows: carbamidomethyl cysteine as fixed modification by the treatment with iodoacetamide, oxidized methionines as variable modification, peptide mass tolerance of 80 ppm, and one missed cleavage site. In all protein identifications, the probability Mowse scores were greater than the minimum score fixed as significant (78 in all cases) with a *p* value less than 0.05.

Yeast Two-hybrid Assay—DGKζ constructs were subcloned in pGBKT7 vector fused to GAL4BD as bait, and SNX27ΔRA was subcloned into pGADT7 vector fused to GAL4AD. The interaction assay was developed according to the manufacturer's protocols (Clontech). The AH109 yeast strain was co-transformed by the LiAc method with pGADT7SNX27ΔRA with each of the DGKζ constructs or with control empty vector. To select co-transformed yeast, cells were plated on SD medium lacking leucine and tryptophan. Growing colonies were replated on high stringency SD medium lacking leucine, tryptophan, alanine, and histidine plus 5-bromo-4-chloro-3-indolyl-α-D-galactopyranoside (X-α-gal) to confirm interacting proteins.

Subcellular Fractionation—We performed subcellular fractionation of Jurkat cells as described previously (38). Briefly 3×10^7 Jurkat cells in logarithmic growth phase were washed twice with PBS at 4 °C and harvested by centrifugation. Cells were resuspended in homogenization buffer A (250 mM sucrose, 20 mM Hepes, pH 7.4, 1 mM EDTA, leupeptin, pepstatin, aprotinin, 50 mM NaF, 50 mM glycerophosphate, 1 mM orthovanadate, and 1 mM PMSF) and then disrupted using a 23-gauge needle. Whole cells and nuclei were removed by centrifugation (800 × *g*, 10 min, 4 °C). All subsequent manipulations were performed at 4 °C. The postnuclear supernatant was centrifuged (20,000 × *g*, 20 min, 4 °C), and the high density microsome fraction was pelleted from the resulting supernatant by centrifugation (45,000 × *g*, 30 min, 4 °C). Low density microsomes were collected from the resulting supernatant by further centrifugation (180,000 × *g*, 90 min, 4 °C). The supernatant from this last centrifugation contained the cytosolic fraction. The pellet resulting from the 20,000 × *g* centrifugation contained the crude plasma membrane; it was collected and resuspended in buffer A, overlaid on 1 ml of 35% sucrose prepared in buffer A, and then centrifuged (100,000 × *g*, 1 h). The purified plasma membrane was collected from the top of the interphase, mixed with buffer B (buffer A without sucrose), and concentrated by centrifugation (108,000 × *g*, 40 min, 4 °C). All pellets were resuspended in the same volume of buffer A using a 25-gauge needle. Samples were analyzed by SDS-PAGE, loading the same volume for each fraction (the cytosol sample represented 1/25 of the total cytosol).

Immunoprecipitation and Western Blot—Jurkat or HEK293 cells, transiently transfected with selected plasmids, were lysed in Nonidet P-40 buffer and cleared by centrifugation. Protein lysates (400 μg) were incubated with the indicated antibodies (2 μl, 1 h, 4 °C) followed by G protein coupled to Sepharose (1 h, 4 °C). Immunoprecipitated complexes were washed, and proteins were separated by 7.5% SDS-PAGE, transferred to nitrocellulose membrane, incubated with appropriate antibodies, and developed using the ECL detection kit (Amersham Biosciences). For immunoprecipitation of endogenous DGKζ, Jurkat cells were lysed in buffer containing 50 mM Tris-HCl, pH 7.5, 150 mM NaCl, 0.1% Triton X-100, and protease inhibitors. Protein lysates (1 mg) were precleared for 30 min using 50 μl of blocked G protein-Sepharose, and the supernatants were incubated with anti-DGKζ Ab overnight at 4 °C. The immunoprecipitated proteins were collected using G protein coupled to Sepharose (2 h, 4 °C) and washed three times with washing buffer. Immunoprecipitated complexes were separated by 10% SDS-PAGE, transferred to nitrocellulose membrane, incubated with appropriate antibodies, and developed using the ECL detection kit (Amersham Biosciences).

Immunofluorescence and Confocal Microscopy—At 24 h post-transfection, cells were transferred to poly(DL-lysine)-coated coverslips and allowed to attach for 30 min. Where indicated, attached cells were treated with wortmannin (10 μM, 1 h, 37 °C) or serum-starved for 30 min and then incubated with Tf-Rhod (20 μg/ml, 15–30 min, 37 °C). Cells were then fixed in cold methanol and washed with PBS. Primary antibodies (diluted 1:100 in PBS with 3% FCS) were incubated (1 h, 37 °C) and washed with PBS; the same procedure was followed for secondary antibodies. Cells mounted on glass slides were imaged with an Olympus Fluoview FV-1000 laser-scanning confocal microscope. A 488 nm krypton-argon laser line was used to record images

of GFP-coupled proteins and Alexa 488 staining, 543 nm helium-neon was used for Cy3 and Tf-Rhod, and 633 nm helium-neon was used for Cy5. Images were processed using Adobe Photoshop software.

Small Interfering RNA of DGKζ—A 64-bp double strand DNA oligonucleotide encompassing an interfering 21-nucleotide sequence of human DGKζ (2290–2310) and a hairpin structure were cloned in the pSUPER (pSUPER-RNAiDGKζ) and the pSUPERGFP (pSUPERGFP-RNAiDGKζ) vectors (Oligoengine). We previously used this sequence to down-regulate DGKζ in HEK293 cells (20). The pSUPER constructs were transfected in Jurkat cells by electroporation. Cell samples were collected from days 1 to 5 post-transfection, and DGKζ levels were evaluated by Western blot (WB) to select the optimal time (96 h) of DGKζ down-regulation. In the case of the pSUPERGFP construct, GFP-positive Jurkat cells were isolated by sorting (Altra Hypersor, Beckman Coulter). pSUPER empty vectors or pSUPER constructs coding scrambled small interfering RNA were used as controls.

Transferrin Recycling—Recycling experiments were as described previously (39–41) with some modifications. Briefly cells were incubated in serum-free medium containing 0.1% BSA (1 h, 37 °C) to remove residual transferrin and then transferred to 4 °C. After 10 min, cells were seeded on poly(DL-lysine)-coated coverslips where samples were labeled (25 min) with 20 μg/ml Tf-Rhod in the assay medium. Cells were then washed twice with cold assay medium to remove uninternalized Tf-Rhod, and one aliquot was maintained at 4 °C in cold serum-supplemented medium as control. The remaining cells were incubated in serum-supplemented medium at 37 °C for different time periods to measure Tf-Rhod recycling as the loss of cell-associated fluorescence. At indicated times, samples were fixed with cold methanol, and cells with pericentriolar Tf-Rhod were counted by confocal microscopy analysis (TCS-NT, Leica, Wetzlar, Germany). z series optical sections (1.25 μm) were recorded. Four contiguous optical sections were stacked using ImageJ software and contained all the three-dimensional fluorescence information. All images were acquired with invariable adjusted laser beam and photomultipliers. We calculated the percentage of cells with pericentriolar Tf-Rhod relative to total cell number (registered in bright field images).

RESULTS

Identification of SNX27 by MS Analysis of DGKζ-associated Proteins—To identify DGKζ-interacting proteins, we generated plasmids encoding full-length (FL) DGKζ or a C-terminal (CT) region of the protein (encompassing the Ank repeats and the PDZbm) fused to GST (Fig. 1*A*). HEK293T cells were transfected with each construct or with empty vector, and expression of the fusion proteins was assessed by WB. Both recombinant proteins were recognized by GST Ab and showed the predicted molecular weight (Fig. 1*B*). GST-fused proteins were batch-purified using glutathione-Sepharose beads. After extensive washing, recombinant proteins and their associated proteins were eluted with Laemmli buffer and separated by SDS-PAGE. Coomassie Blue gel staining showed nonspecific bands associated with glutathione-Sepharose in control cells (Fig. 1*C*, *Mock*). DGKζFL and DGKζCT pulled down a ~60-kDa double band that was absent in controls (Fig. 1*C*). Bands were excised from gels and identified by MS (see "Experimental Procedures").

Proteomics analysis of the excised bands with MALDI-TOF showed several peptides matching the SNX27 sequence. SNX27 comprises two variants, *a* and *b*, originally identified as products generated by alternative splicing of the *mrt1* gene in rat. SNX27*a* is expressed constitutively in brain and testis, whereas the *b* isoform is induced in brain following methamphetamine treatment (42). Both isoforms are identical except in their last amino acids, two for the *b* isoform and 13 for the *a* isoform (Fig. 1*D*, *bottom*, *boxed*). For band 1 (Fig. 1*C*), 20 of 28 mass values matched with SNX27*a* (accession number gi:55960553), covering 37% of the protein sequence (Fig. 1*D*, *left*, *underlined*). For band 2 (Fig. 1*C*), 24 of 31 mass values searched matched with SNX27*b* sequence (accession number gi:31742501), spanning 44% of the full-length protein (Fig. 1*D*, *right*, *underlined*). In both cases, experimentally measured peptides masses were compared with the theoretical SNX27 sequences using FindMod software package from ExPASy Proteomics Server (www.expasy.org). This analysis showed that one of the experimental peptides corresponding to band 1 matched exclusively with the SNX27*a* sequence; this peptide was within the last 13-amino acid sequence specific to this splice variant.

SNX27 belongs to the large sorting nexin protein family defined by the presence of a PX domain, characteristic of interaction with 3-phosphorylated derivatives of phosphatidylinositol (PI) (43–47). The SNX protein family is proposed to regulate intracellular trafficking (30, 31).

DGKζ Interacts with SNX27a and -b in HEK293 Cells—SNX27 is the only member of the SNX family that, in addition to the PX domain, has a Ras association (RA) domain and a class I PDZ domain. It is noteworthy that SNX27 was pulled down with DGKζ constructs with a common C-terminal region containing a PDZbm; this prompted us to analyze the requirement for the DGKζ PDZbm in this interaction.

HEK293 cells were transfected with empty vector, DGKζFL, or a DGKζ mutant with deletion of the C-terminal PDZbm (DGKζΔPDZbm) fused to a Myc tag (Fig. 2*A*). Ectopically expressed proteins were immunoprecipitated with an anti-Myc Ab, and association of endogenous SNX27 was determined by WB. The SNX27 Ab revealed a double band both in lysates and in DGKζFL immunoprecipitates but not in DGKζΔPDZbm immunoprecipitates (Fig. 2*B*). This doublet probably corresponds to the two SNX27 splice variants (42), although the existence of post-translational protein modifications such as phosphorylation cannot be excluded. We further analyzed DGKζ association with each SNX27 isoform independently by co-immunoprecipitation of the overexpressed proteins. HEK293 cells were co-transfected with GFP-fused SNX27*a* and with Myc-fused DGKζFL, DGKζΔPDZbm, or control empty plasmid (Fig. 2*C*). Immunoprecipitation with anti-Myc Ab showed association of ectopically expressed SNX27*a* in DGKζFL but not in DGKζΔPDZbm immunoprecipitates (Fig. 2*C*). Similar data were obtained when GFP-fused DGKζ constructs or control vector was co-transfected with Myc-tagged SNX27*b*, immunoprecipitated with anti-GFP, and developed using anti-Myc and anti-SNX27 Abs (Fig. 2*D*); as shown, a doublet corresponding to endoge-

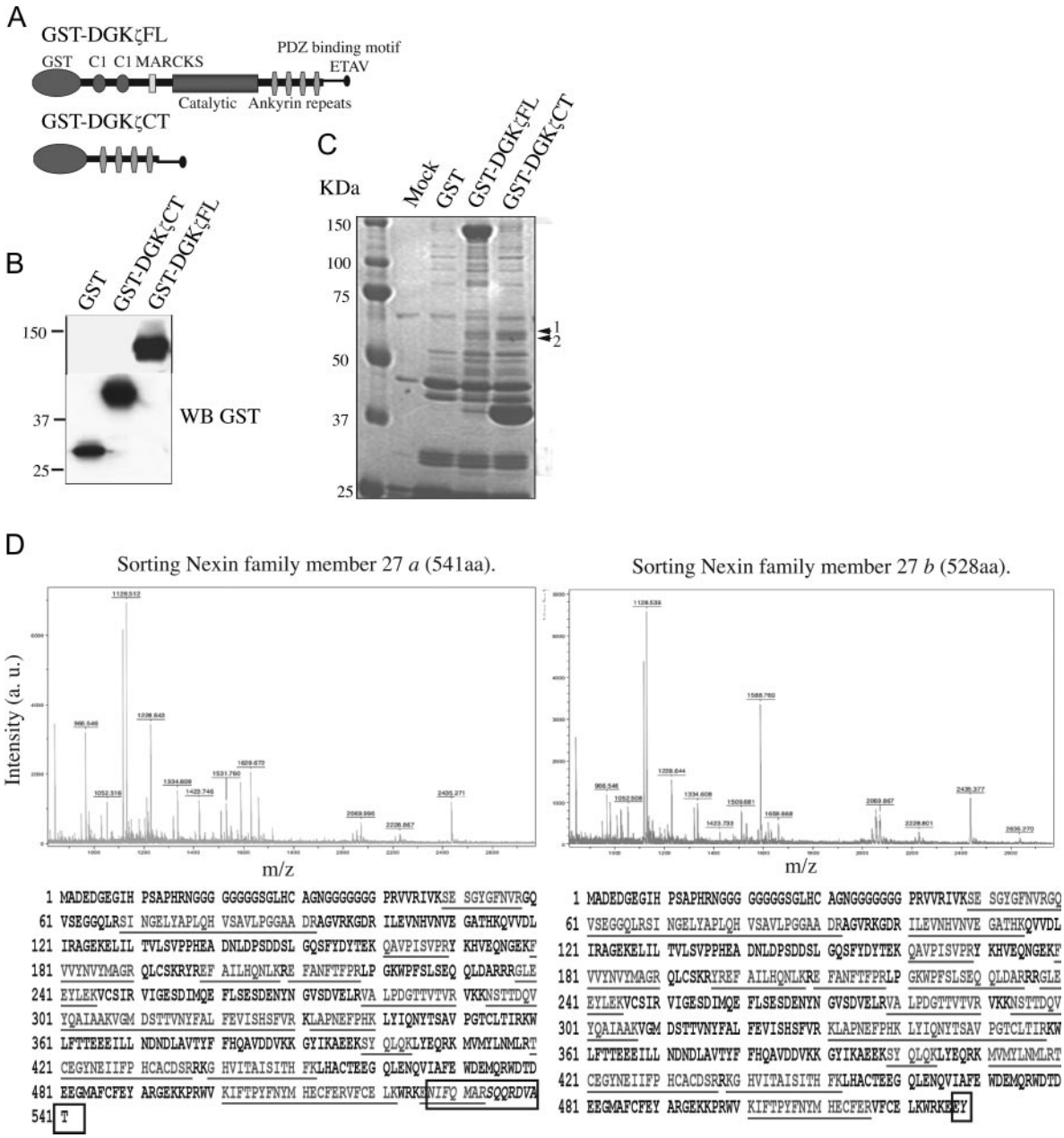

FIG. 1. **Proteomics identification of SNX27 as a DGKζ binding partner.** *A*, the FL or the CT region of DGKζ (including four Ank repeats and a PDZbm) were fused to GST tag. Conserved motifs are indicated. *B*, HEK293T cells were transfected with constructs or empty vector and processed 24 h later for WB. Analysis with anti-GST Ab showed proteins of the predicted molecular weight. *C*, HEK293T cells were transfected with the indicated plasmids, harvested, lysed, incubated with glutathione-Sepharose, and washed (see "Experimental Procedures"). Bound proteins were eluted, separated by SDS-PAGE, and Coomassie Blue-stained. The indicated bands (*1* and *2*) were excised from the gel, trypsin-digested, and analyzed by MS. *D*, MALDI-MS spectrum of the tryptic peptides identified in the ~60-kDa double band from the DGKζ-interacting proteins (*top*). Both bands were subjected to in-gel trypsin digestion, and resulting peptides were analyzed by MALDI-MS. Mass value (*m/z*) and putative amino acid position assignments are indicated *above* peaks; assignments were made using Mascot software. The peptide coverage map of the proteins identified is shown (*bottom*). The peptide coverage map of the proteins identified is shown *underlined*. *Boxed* amino acids (*aa*) represent the differences between *a* and *b* isoforms.

nous and ectopically expressed SNX27 was found only when we used anti-SNX27 Ab. These results demonstrate that the DGKζ PDZbm is indispensable for its interaction with SNX27 isoforms.

To further assess the requirement of the SNX27 conserved domain for interaction with DGKζ, we co-expressed Myc-tagged SNX27*b* constructs bearing different deletions (Fig. 2*E*) and GFP-tagged DGKζFL or GFP control and immunoprecipitated with anti-GFP Ab. SNX27*b* was not detected in control anti-GFP pellets (not shown). All SNX27 recombinant

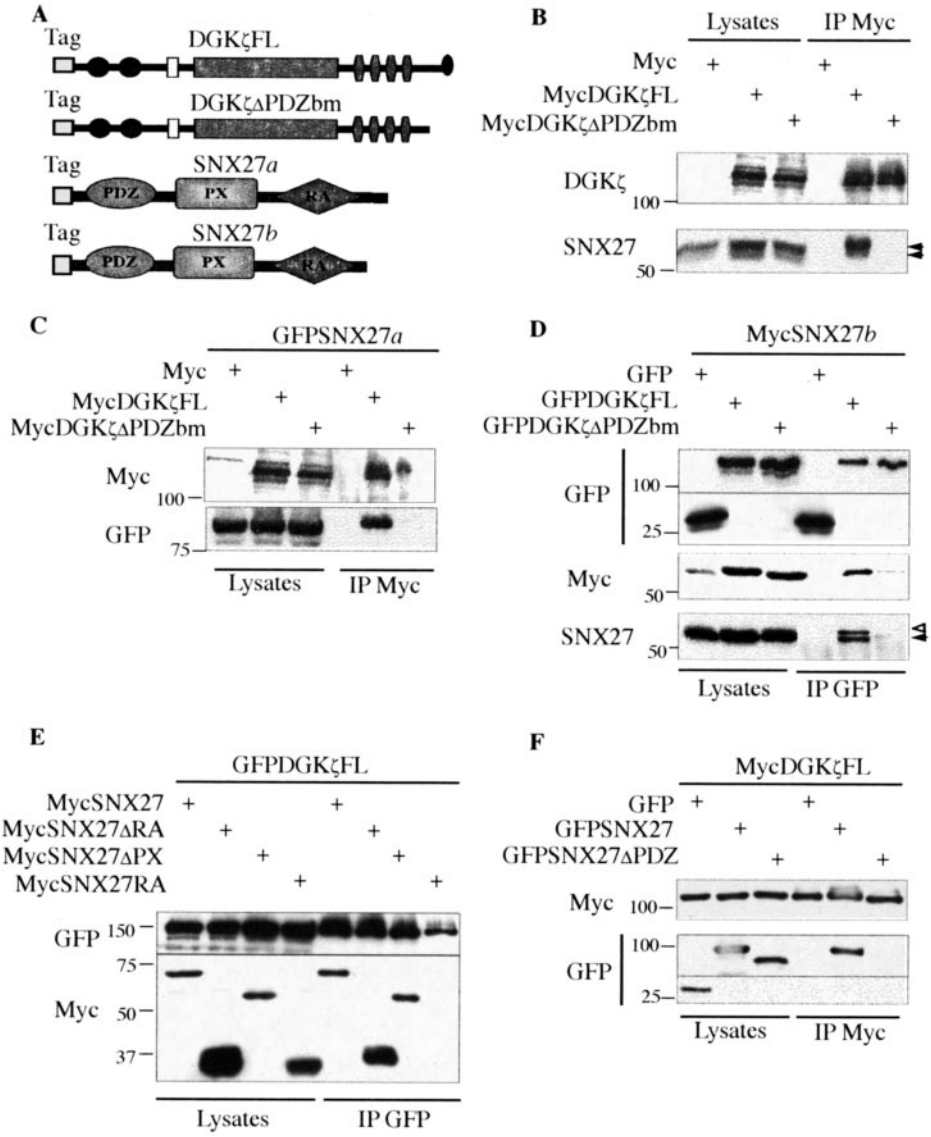

FIG. 2. **DGKζ interacts with SNX27*a* and SNX27*b* in a PDZ-dependent manner in HEK293 cells.** *A*, constructs used for the experiments include DGKζFL, a deletion mutant of the PDZbm (DGKζΔPDZbm), SNX27*a*, and SNX27*b*. *B*, HEK293 cells were transfected with Myc-tagged DGKζ constructs; after 24 h, total cell lysates were immunoprecipitated with anti-Myc Ab and proteins were separated by SDS-PAGE and analyzed by WB using anti-DGKζ (*top*) or -SNX27 Ab (*bottom*). SNX27 signals coincide with the molecular weights in Coomassie Blue-stained gels (see Fig. 1*C*). *C*, HEK293 cells were co-transfected with GFP-SNX27*a* and the indicated Myc-tagged DGKζ constructs; after 24 h, cell lysates were immunoprecipitated with anti-Myc Ab. Proteins were resolved, and the indicated proteins were developed in WB using anti-Myc (*top*) and -GFP Ab (*bottom*). *D*, HEK293 cells were co-transfected with Myc-SNX27*b* and the indicated GFP-DGKζ constructs; after 24 h, cell extracts were immunoprecipitated with anti-GFP Ab, immunoprecipitates were resolved by SDS-PAGE, and the indicated proteins were developed in WB using anti-GFP (*top*) and anti-Myc Abs (*middle*). Transfected and endogenous SNX27 were identified with anti-SNX27 Ab (*bottom*). In *B* and *D*, DGKζ, but not DGKζΔPDZbm, associated with both endogenous (*solid arrowhead*) and ectopically expressed SNX27 (*open arrowhead*). *E*, HEK293 cells were co-transfected with GFP-DGKζ and Myc-SNX27 constructs bearing deletions of different domains; after 24 h, we determined the presence of the constructs in DGKζ immunoprecipitates by WB using anti-GFP (*top*) and -Myc Abs (*bottom*). *F*, HEK293 cells were co-transfected with Myc-DGKζ and GFP, GFP-SNX27*a*, or a mutant bearing a deletion of the PDZ domain (*GFPSNX27ΔPDZ*). SNX27 in anti-Myc immunoprecipitates was assessed as in *E*. In *E* and *F*, only the SNX27 construct with an intact PDZ domain was able to associate with DGKζ. All experiments were repeated three times with similar results. Input (*Lysates*) represents 5% of starting material. *IP*, immunoprecipitate.

proteins with an intact PDZ domain co-immunoprecipitated with DGKζ (Fig. 2*E*). In contrast, the SNX27 mutant bearing a PDZ domain deletion was not found in DGKζ immunoprecipitates (Fig. 2*F*). All together, these results show that DGKζ interacts, through its C-terminal PDZbm, with the PDZ domain of constitutive and inducible SNX27 forms.

Direct PDZ-mediated Interaction of SNX27 with DGKζ—Co-immunoprecipitation experiments suggested direct interac-

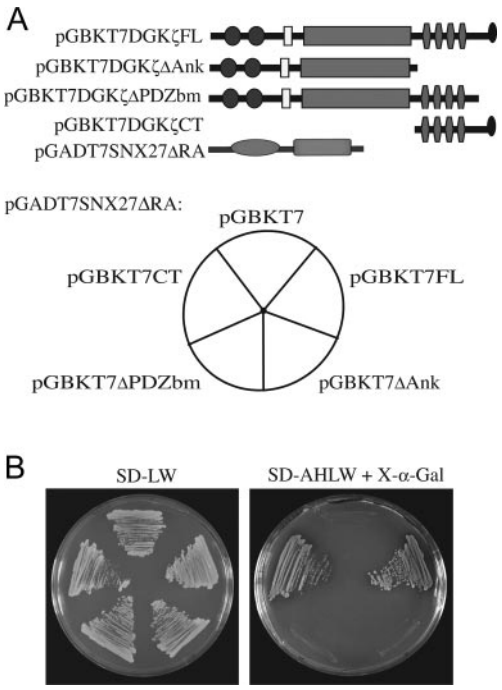

FIG. 3. **Characterization of the DGKζ-SNX27 interaction using the yeast two-hybrid system.** *A*, four DGKζ constructs were subcloned in the pGBKT7 vector fused to GAL4BD. The N-terminal region of SNX27 (containing the PDZ and PX domains) was subcloned in pGADT7 fused to GAL4AD (*top*). The AH109 yeast strain was co-transformed with pGADT7SNX27ΔRA and the indicated DGKζ constructs or control empty vector (*bottom*). *B*, co-transformed yeast were plated on leucine- and tryptophan-free SD medium (*SD−LW*, left). To confirm interacting proteins, co-transformed yeast were grown on highly stringent medium lacking leucine, tryptophan, alanine, and histidine (*SD−AHLW*) plus X-α-Gal (*right*).

tion between DGKζ and SNX27. To rule out the possible participation of an intermediate protein, we analyzed the DGKζ-SNX27 interaction by yeast two-hybrid assays. Four DGKζ constructs encompassing different portions of the protein were subcloned in the pGBKT7 vector fused to the GAL4BD, whereas SNX27ΔRA was subcloned in pGADT7 (Fig. 3*A*, *top*). All constructs were analyzed for normal protein expression in yeast (not shown). pGADT7SNX27ΔRA was co-transformed in the AH109 yeast strain with each DGKζ construct or empty pGBKT7 as control (Fig. 3*A*, *bottom*). Cells were grown on SD medium lacking leucine and tryptophan (Fig. 3*B*, *left*); co-transformed yeast were then plated on highly stringent SD medium lacking leucine, tryptophan, adenine, and histidine plus X-α-Gal (Fig. 3*B*, *right*). Those DGKζ constructs lacking the complete CT region (ΔAnk) or the PDZbm (ΔPDZbm) were unable to interact with SNX27ΔRA, whereas strong interaction was observed for the constructs encoding the complete protein or the CT region (Fig. 3*B*, *right*). These results strongly suggest the direct association of DGKζ and SNX27 via PDZ interaction.

SNX27 Is Expressed in Cells of Hematopoietic Origin—Previous studies using rat tissues have shown that mRNAs for SNX27*a* and -*b* are expressed predominantly in brain and testis (42), but protein expression has not been fully assessed. We investigated expression of endogenous SNX27 in hematopoietic cells. WB analysis in distinct cells of hematopoietic origin demonstrated SNX27 expression in all cell types evaluated (Fig. 4*A*).

We performed new co-immunoprecipitation assays to determine whether ectopically expressed SNX27 also associated with DGKζ in Jurkat T lymphocytes as it does in HEK293 cells. Cells were co-transfected with plasmids expressing GFP (control) or GFP-SNX27 and Myc-tagged DGKζFL, DGKζΔPDZbm, or empty plasmid. Analysis of Myc immunoprecipitates showed that both endogenous and ectopically expressed SNX27 associated exclusively with DGKζFL but not with DGKζΔPDZbm (Fig. 4*B*). These results confirm that the PDZ-specific interaction between SNX27 and DGKζ is also found in T lymphocytes.

Analysis of endogenous protein interaction was largely impaired by the lack of suitable antibodies. Although the anti-SNX27 Ab was very efficient in WB, it bound the PDZ region, making immunoprecipitation-based assessment of PDZ-mediated interaction impossible. This is also true for most anti-DGKζ Abs, which were specific for a C-terminal peptide encompassing the ETAV sequence that mediates SNX27 interaction. Immunoprecipitation experiments were thus performed with an Ab raised against the DGKζ N-terminal domain; albeit not very efficient, this Ab permitted detection of a weak band with a molecular weight corresponding to that of SNX27 (Fig. 4*C*). Detailed analysis of the interaction of the endogenous proteins must thus await the generation of improved tools for immunoprecipitation.

As an alternative approach to assess co-localization of endogenous proteins, we examined the subcellular expression pattern of both proteins in different T lymphocyte fractions. The cytosolic fraction contained very low levels of DGKζ, whereas SNX27 and EEA1 were abundantly found suggesting, as described previously (46), that binding to 3-phosphorylated PI does not sustain recruitment to endosomes. DGKζ was absent from the plasma membrane fraction where a very faint SNX27 band was observed. SNX27 co-localized with DGKζ in internal membrane fractions corresponding to high and low density microsomes (Fig. 4*D*), suggesting interaction between these proteins at these subcellular localizations.

PX and PDZ Domains Are Responsible for SNX27 Vesicular Association in T Lymphocytes—As the fractionation experiments indicated no specific SNX27 location, we examined its exact localization in intact cells. Immunofluorescence (IF) analysis of Jurkat T cells showed that endogenous SNX27 localized to cytosol with accumulation in vesicular structures (Fig. 5*A*). To analyze the role of SNX27 domains in the subcellular localization of this protein, we generated several deletion mutants, which we transfected into Jurkat T cells and analyzed by IF. The subcellular localization pattern of Myc-

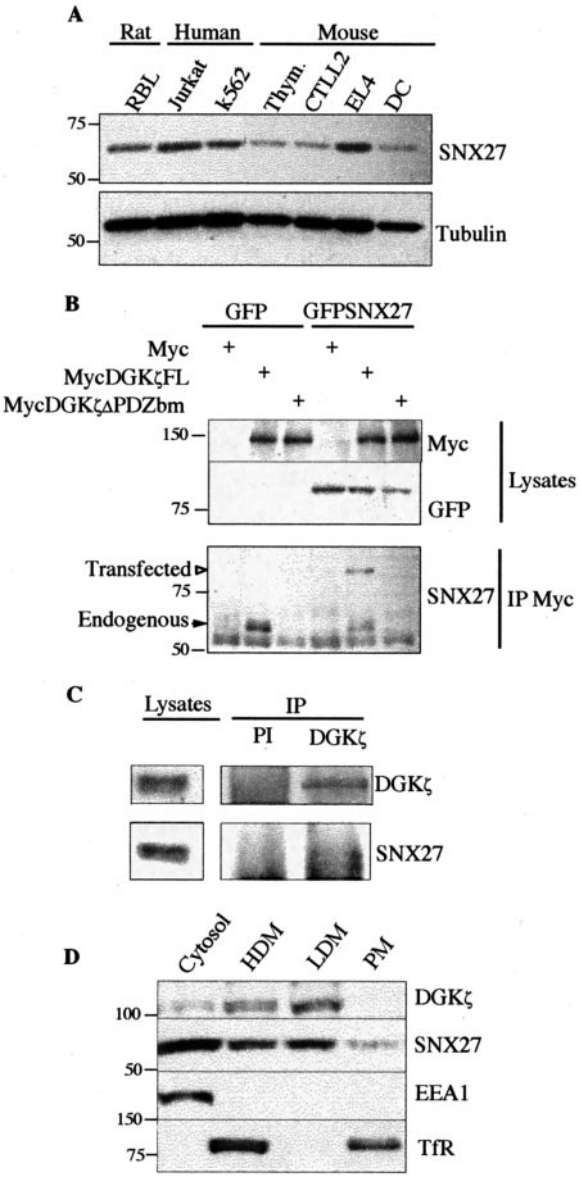

FIG. 4. **SNX27 is expressed in cells of hematopoietic origin.** *A*, different hematopoietic cell types were lysed, separated by SDS-PAGE, and analyzed by WB with anti-SNX27 Ab; anti-tubulin Ab was used as loading control. *RBL*, rat mast cell line; *Jurkat*, human acute T cell leukemia; *K562*, human chronic myelogenous leukemia; *CTLL2*, mouse cytotoxic cell line; *EL4*, mouse T lymphoma; *Thym.*, mouse thymocytes; *DC*, mouse dendritic cells. *B*, Jurkat T cells were co-transfected with GFP or GFP-SNX27 and either Myc-DGKζ or a mutant lacking the PDZbm, and cells were processed as in Fig. 2. Myc-DGKζ but not Myc-DGKζΔPDZbm immunoprecipitates showed association of endogenous (*solid arrowhead*) and ectopically expressed SNX27 (*open arrowhead*). *C*, Jurkat cell lysates were immunoprecipitated with either preimmune (*PI*) serum or with an anti-DGKζ Ab to the N-terminal domain of the protein, and endogenous SNX27 was assessed in the immunoprecipitates as described in Fig. 2. Lysates represent 5% of starting material. *D*, subcellular fractions of Jurkat T cells were purified by high speed centrifugation (see "Experimental Procedures"), and the presence of DGKζ and SNX27 was determined in WB with appropriate antibodies. *IP*, immunoprecipitate; *HDM*, high density microsome fraction; *LDM*, low density microsome fraction.

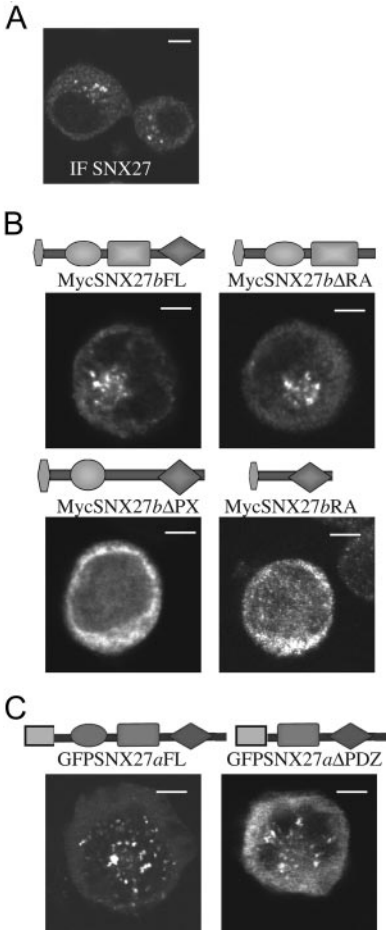

FIG. 5. **Vesicular targeting of SNX27 in Jurkat T cells is PX and PDZ domain-dependent.** *A*, Jurkat T cells were fixed and then stained with rabbit anti-SNX27 Ab followed by anti-rabbit IgG-Alexa 488. *B*, Jurkat T cells were transfected with the indicated Myc-SNX27*b* constructs; after 24 h, cells were fixed and stained for IF using anti-Myc and anti-mouse IgG-Cy3 antibodies. Myc-SNX27FL and Myc-SNX27ΔRA showed a punctate pattern that accumulated in a specific cytosolic location, whereas Myc-SNX27ΔPX and Myc-SNX27RA did not localize in vesicles. *C*, Jurkat T cells were transiently transfected with a GFP-SNX27 construct or a mutant with deletion of the PDZ domain (GFP-SNX27ΔPDZ). After 24 h, cells were fixed and analyzed by confocal microscopy. The GFP-SNX27 construct showed the same expression pattern as the endogenous protein; GFP-SNX27ΔPDZ showed less vesicle localization than the FL counterpart. *Bars*, 3 μm.

tagged SNX27*b* (MycSNX27FL) and of a mutant lacking the RA domain (MycSNX27ΔRA) was similar to that of the endogenous protein, suggesting that the RA domain is not necessary for vesicular localization (Fig. 5*B*, *top*). Vesicle colocalization was lost following deletion of the PX domain (MycSNX27ΔPX) as was also the case when the RA domain was expressed alone (MycSNX27RA) (Fig. 5*B*, *bottom*). A fusion protein N-terminally labeled with GFP showed vesicular distribution similar to that of the endogenous protein (Fig. 5*C*), and vesicle colocalization was partially lost after PDZ deletion (GFPSNX27ΔPDZ) (Fig. 5*C*). The data confirm that the SNX27

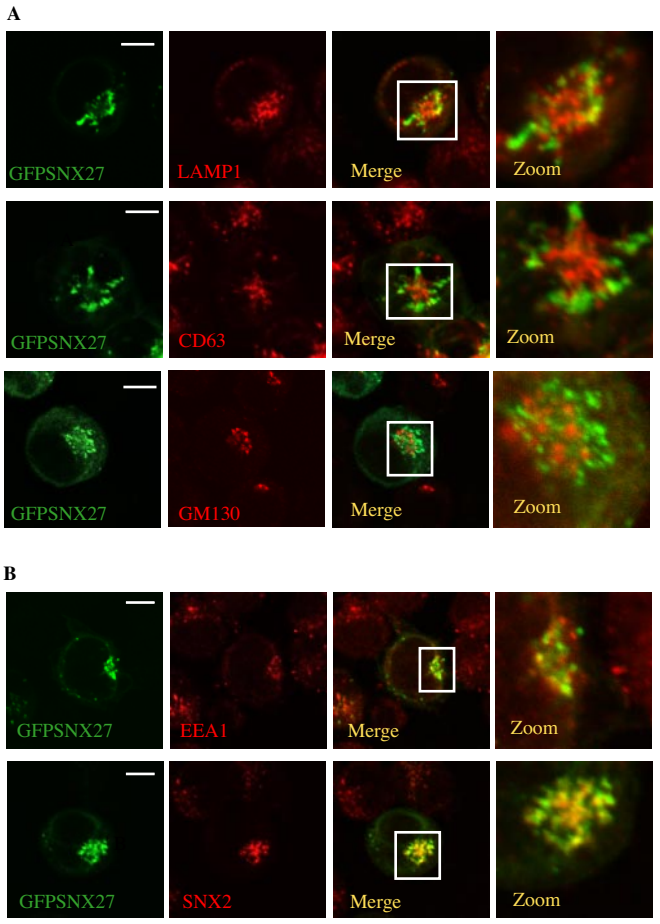

FIG. 6. **SNX27 is found in sorting endosomes in Jurkat T cells.** Cells were transfected with GFP-SNX27, fixed after 24 h, and processed for labeling of vesicular markers with primary Ab followed by anti-mouse IgG-Cy3 antibodies. *A*, LAMP1 and CD63 were used to label late endosome/lysosome and immature vesicles (*top* and *middle rows*, respectively); GM130 was used to detect *cis*-Golgi (*bottom row*). Merged images (*third column*) are magnified to show detail (*fourth column*). None of these vesicular markers co-localized with GFP-SNX27. *B*, EEA1 (*top row*) or SNX2 Ab (*bottom row*) were used to stain sorting endosomes. *Yellow* staining indicates co-localization of GFP-SNX27 and the vesicular markers. Note that GFP-SNX27 co-localized with both markers but that some additional GFP-SNX27-labeled vesicles were negative for sorting endosome staining. *Bars*, 3 μm.

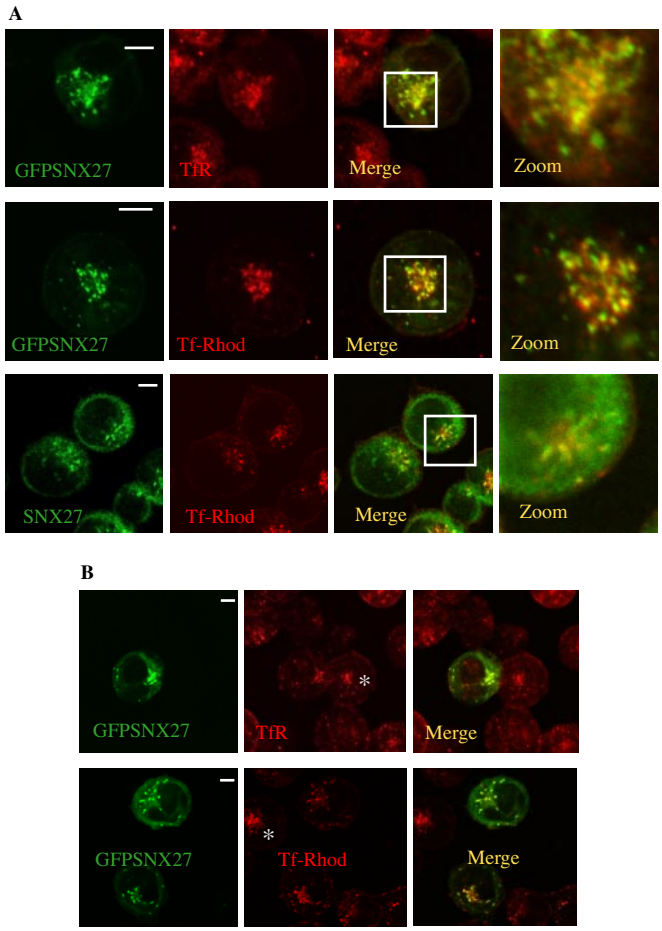

FIG. 7. **SNX27 association with the endocytic recycling system in Jurkat T cells.** *A*, at 24 h post-transfection with GFP-SNX27, cells were fixed and stained with anti-TfR Ab followed by anti-mouse IgG-Cy3 Ab (*top row*) or were treated with 20 μg/ml Tf-Rhod, then fixed, and analyzed by confocal microscopy (*middle row*). Untransfected Jurkat T cells were Tf-Rhod-treated, fixed, and then stained with anti-SNX27 and anti-rabbit IgG-Alexa488 Abs (*bottom row*). Merged images (*third column*) are magnified to show detail (*fourth column*). Immunofluorescence analyses showed strong co-localization (*yellow*) between SNX27 and TfR/Tf-Rhod. *B*, Jurkat T cells were processed 24 h after GFP-SNX27 transfection for staining with anti-TfR (*top*) or were treated with Tf-Rhod (*bottom*) as in *A*. Untransfected control cells are indicated with an *asterisk*. Immunofluorescence analysis revealed no specific TfR or Tf-Rhod accumulation in cells overexpressing GFP-SNX27.

PX domain is indispensable for its vesicular location, as reported for other SNX family members (46), and demonstrate that vesicle localization of SNX27 is not as efficient without an intact PDZ domain.

SNX27 Is Present in the Recycling Endocytic Pathway in T Lymphocytes—The SNX family members are proposed to participate in various aspects of endocytosis and membrane trafficking. Endocytic pathways control the internalization of extracellular components, a mechanism that is essential in the regulation of diverse signal transduction pathways. The best characterized endocytic process is receptor-mediated endocytosis, which involves receptor internalization by clathrin-coated vesicles. Receptors are delivered to sorting endosomes, which can follow one of at least three pathways. One is the prodegradative pathway through late endosomes and lysosomes, another is the Golgi network, and the third is the endocytic recycling pathway in which receptors can return to the cell surface directly or through the endocytic recycling compartment (ERC) (30, 31).

To elucidate the exact nature of the SNX27-positive vesicles, we performed co-localization analyses of GFP-SNX27 with markers specific for each sorting pathway. We used

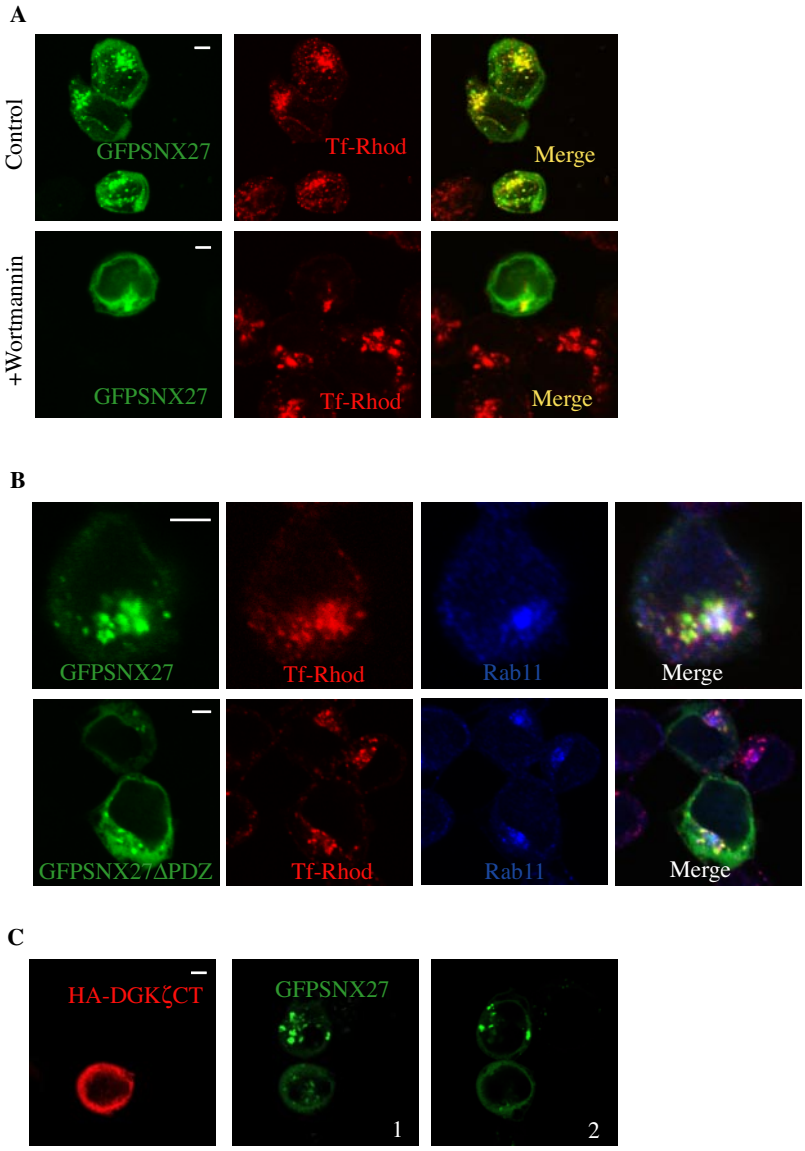

FIG. 8. **Vesicle association of SNX27 is wortmannin-sensitive and requires DGKζ interaction.** *A*, Jurkat T cells were transfected with GFP-SNX27; after 24 h, cells incubated with Tf-Rhod were treated with 10 μM wortmannin and then fixed for immunofluorescence analysis. Vesicular GFP-SNX27 localization was lost after wortmannin treatment, resulting in diffuse cytosolic staining. *Bars*, 3 μm. *B*, Jurkat cells were transfected with GFP-SNX27 or GFP-SNX27ΔPDZ; after 24 h, cells were treated with 20 μg/ml Tf-Rhod, fixed, and stained with anti-Rab11 followed by anti-rabbit IgG-Cy5 Ab. GFP-SNX27, *green*, *first column*; Tf-Rhod, *red*, *second column*; Rab11, *blue*, *third column*. In merge images (*fourth column*), *yellow* staining indicates GFP-SNX27 and Tf-Rhod co-localization, *purple* staining shows Tf-Rhod and Rab11 co-localization, and *cyan* indicates GFP-SNX27 and Rab11 co-localization. *White* merge signal shows GFP-SNX27, Tf-Rhod, and Rab11 co-localization. *Bars*, 3 μm. *C*, Jurkat cells were co-transfected with GFP-SNX27 and a plasmid encoding the CT region of DGKζ fused to an HA tag. 24 h after transfection cells were fixed and stained with anti-HA Ab followed by anti-mouse IgG-Cy3. The reduced vesicle localization of SNX27 in cells expressing both proteins is compared with its localization in cells not expressing the HA-DGKζ construct. (*1* and *2* are two different optical z sections.)

LAMP1 and CD63 as late endosome/lysosome markers (48, 49) (Fig. 6*A*, *top* and *middle rows*) and GM130 as a *cis*-Golgi marker (50) (Fig. 6*A*, *bottom row*). SNX27 did not co-localize with any of these markers (Fig. 6*A*, *third* and *fourth columns*), indicating that it is absent from late endosomes/lysosomes and the Golgi network. In contrast, SNX27 clearly co-localized with proteins of the sorting endosomes, such as EEA1 (51) (Fig. 6*B*, *top row*) and SNX2, another sorting nexin reported to associate with sorting endosomes (52) (Fig. 6*B*, *bottom row*). Higher magnification revealed that, in addition to co-localization with sorting endosomes, GFP-SNX27 was present in other vesicles (Fig. 6*B*, *fourth column*). We thus analyzed SNX27 co-localization with TfR, one of the best characterized proteins in the endocytic recycling pathway (53). SNX27 co-localized extensively with steady-state intracellular TfR, suggesting that SNX27 is enriched in the vesicles that transport this receptor (Fig 7*A*, *top row*). The TfR can also be tracked by labeling with Tf-Rhod. SNX27 co-localization with Tf-Rhod (Fig. 7*A*, *middle row*) confirmed that SNX27 localizes in the endocytic recycling pathway in T lymphocytes. Results were similar when endogenous SNX27 was analyzed (Fig. 7*A*, *bottom row*). Overexpression of some SNXs may perturb endosomal structures, leading to increased TfR staining, thereby artificially affecting receptor trafficking (46). To test whether SNX27 overexpression altered transferrin transport through the endocytic recycling pathway, we compared GFP-SNX27-transfected *versus* control cells (Fig. 7*B*). We found no differences in accumulation of TfR (*top*) or Tf-Rhod (*bottom*), suggesting that SNX27 overexpression does not alter endosomal structures in this system.

Phosphoinositide-3-OH Kinase (PI3K) Activity and DGKζ Interaction Regulate SNX27 Binding to Vesicles in T Lymphocytes—Previous experiments indicated a role for SNX27 PX

and PDZ domains in vesicle localization of the protein. SNX27-positive vesicles co-localized extensively with steady-state intracellular TfR, suggesting that SNX27 is enriched in the vesicles that transport this receptor. The products of PI3K may target PX-containing proteins to specific subcellular locations. To study the 3-phosphorylated PI requirement in SNX27 vesicular localization, we examined GFP-tagged SNX27/Tf-Rhod distribution in Jurkat T cells treated with the PI3K inhibitor wortmannin (54). Under this treatment, endosomal structures were profoundly modified, and GFP-SNX27 redistributed promptly to cytosol (Fig. 8*A*), confirming that SNX27 vesicular association depends on PI3K products.

Rab11 is a small GTPase localized in the ERC that is essential for TfR transport to the membrane (55, 56). To confirm SNX27 participation in the endocytic recycling pathway and to further assess the role of the SNX27 PDZ domain in the subcellular localization of this protein, we determined SNX27 or SNX27ΔPDZ and Rab11 localization in Tf-Rhod-treated cells. GFP-SNX27 clearly co-localized with the Tf-Rhod- and Rab11-positive structures (Fig. 8*B*). SNX27ΔPDZ and Rab11 fluorescent signal overlap was less pronounced, suggesting that lack of this domain prevented enrichment of SNX27 in TfR-containing vesicles.

These experiments support our observations with deletion mutants, showing that although the PX domain is essential for SNX27 binding to vesicles the PDZ domain is also required for efficient association. To further study DGKζ participation in SNX27 binding to vesicles, we disrupted interaction with endogenous DGKζ by overexpressing its C-terminal domain. A construct encompassing the DGKζ Ank repeats and PDZbm showed no specific localization (Fig. 8*C*). SNX27 binding to vesicles was diminished in cells expressing this construct, suggesting that disruption of interaction with endogenous DGKζ affected SNX27 binding to vesicles (Fig. 8*C*).

DGKζ Depletion in Jurkat T Cells Accelerates TfR Exit from the ERC—Our studies demonstrated that, in T cells, DGKζ interacts with SNX27 and that SNX27 localizes in TfR-positive vesicles. Deletion of the PDZ domain altered SNX27 vesicle co-localization as did overexpression of the DGKζ C-terminal domain. These experiments suggested that SNX27 and DGKζ interaction promotes enrichment of the former in TfR-positive vesicles. Co-localization of endogenous DGKζ with SNX27 and/or TfR-positive vesicles was difficult to determine due to the lack of an anti-DGKζ Ab suitable for IF analysis. In addition, ectopically expressed GFPDGKζ has a broad expression pattern in T lymphocytes, making it difficult to assess its vesicular localization during TfR trafficking. To assess the functional role of the SNX27-DGKζ interaction, we therefore evaluated possible DGKζ function in TfR recycling. We analyzed TfR recycling in T lymphocytes in which DGKζ expression was knocked down using RNA interference (RNAi).

We transfected Jurkat T cells with plasmids encoding a small hairpin RNAi (pSUPER-RNAiDGKζ or pSUPERGFP-RNAiDGKζ) and assessed down-regulation of endogenous protein by WB (Fig. 9*A*). RNAi efficiently down-regulated DGKζ levels expressed in T cells (57). Transfected T cells were labeled with

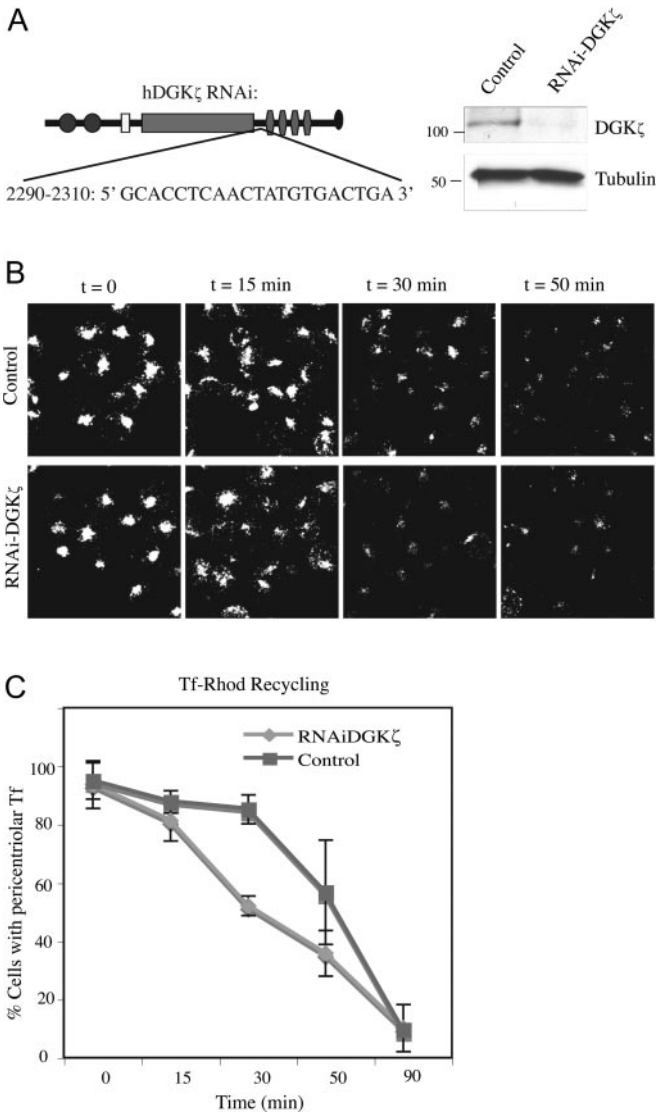

FIG. 9. **DGKζ depletion accelerates the kinetics of Tf-Rhod exit from the ERC.** *A*, a 64-bp double strand DNA oligonucleotide encompassing an interfering 21-nucleotide sequence of human DGKζ (2290–2310) (*left*) and a hairpin structure were cloned in pSUPER. pSUPER (control) or pSUPER-RNAiDGKζ were transfected in Jurkat cells by electroporation. Cell samples were taken 96 h after transfection, and DGKζ levels were evaluated by WB using anti-DGKζ Ab. Anti-tubulin Ab was used as loading control. RNAiDGKζ efficiently decreased DGKζ expression (*right*). *B*, to measure the rate of Tf-Rhod recycling exit from the ERC, Jurkat T cells were transfected with empty plasmid or pSUPER-RNAiDGKζ; after 96 h, cells were treated with Tf-Rhod at 4 °C, washed, and transferred to 37 °C to count the number of cells with pericentriolar Tf-Rhod at different times after sample transfer. *C*, the number of control or DGKζ-knocked down cells with pericentriolar Tf-Rhod, counted at the times indicated, is expressed as a percentage of total cells. Mean ± S.D. is shown for three independent experiments.

Tf-Rhod (see "Experimental Procedures"), and staining was analyzed at different times. Even at time 0 (when cells were transferred from 4 to 37 °C), we observed strong pericentriolar Tf-Rhod staining, suggesting that TfR internalization in Jurkat T cells is very rapid compared with other cell types (39). Exit from the pericentriolar compartment was reflected by loss of fluorescence (Fig. 9*B*). At time 0, pericentriolar staining was similar in controls and cells with down-modulated DGKζ (Fig. 9, *B* and *C*). In contrast, the percentage of pericentriolar Tf-Rhod at 30 and 50 min was lower in cells with diminished DGKζ compared with controls. Similar data were obtained when we enriched the DGKζ-knocked down cell population using the GFP version of the RNAi plasmid. Analysis of three independent experiments indicated that down-regulation of DGKζ protein levels increased the rate of TfR recycling back to the cell surface (Fig. 9, *B* and *C*). These results demonstrate that DGKζ acts as a negative modulator of TfR recycling from ERC to the plasma membrane.

DISCUSSION

DGKζ is expressed ubiquitously, and its functions range from cell cycle regulation to cytoskeletal remodeling and/or regulation of immune function (20–24). DGKζ localization to specialized membrane regions is a general mechanism for its functional regulation, and the presence of well characterized protein-protein interaction domains suggests that DGKζ can participate in various signaling pathways. Using a proteomics approach to detect novel DGKζ-interacting proteins, we identified SNX27. We demonstrated that DGKζ interacts with the SNX27 PDZ domain, and we describe previously unreported functions for this isoform in the regulation of membrane trafficking.

Videomicroscopy studies in living Jurkat T cells showed that DGKζ translocates to the plasma membrane in response to activation of an exogenously expressed muscarinic type I receptor (25). These studies showed that the C-terminal region of the protein confers specificity for DGKζ translocation in response to different receptors, suggesting that membrane localization of DGKζ would require C-terminal region-mediated interaction with specific scaffold proteins (25). This hypothesis was confirmed by reports that identified DGKζ-associated proteins, indicating that PDZ-mediated interaction is central to DGKζ localization to and function in specific membranes (26, 33, 58). In neurons, for instance, PDZ-mediated interaction with syntrophins regulates DGKζ translocation to the plasma membrane where it translates receptor signals into the cytoskeletal rearrangements required for neurite outgrowth (23). The identification of SNX27 as a DGKζ partner reveals a novel PDZ-dependent interaction, suggesting that DGKζ acts in membrane compartments other than the plasma membrane.

The sorting nexin family comprises 29 distinct proteins in mammals and 10 in yeast with roles ranging from prodegradative sorting and internalization to endosomal recycling and/or endosomal sorting (31). This family is characterized by the presence of an SNX PX domain that targets these proteins to 3-phosphorylated PI-enriched membranes. Our experiments demonstrated vesicular localization for both endogenous and ectopically expressed SNX27 in Jurkat T cells similar to SNX27 localization in adherent cells such as A431 (34), HEK293, and HeLa.[2] We also showed that SNX27 depends on its PX domain to localize in TfR-positive vesicles within the sorting endosomes and the ERC. This PX-dependent association was sensitive to wortmannin, confirming that SNX27 subcellular localization has a strict 3-phosphorylated PI requirement as described for other family members (46). In addition, our results showed that the PDZ domain, unique to this SNX isoform, provides additional regulation for vesicle binding. This suggests that PDZ-mediated interactions of SNX27 with protein partners are important for vesicular localization.

Several SNX proteins also have a C-terminal coiled coil region encoding a Bin/amphiphysin/Rvs (BAR) domain (59), which acts as a dimerization and a membrane-binding region, able to sense membrane curvature (60). The presence of both a BAR and a PX domain suggests a complex SNX localization mechanism in which SNX membrane association would be regulated by the degree of physical membrane curvature. Some SNX family members have additional protein-protein interaction domains, including the SH3 (Src homology domain type 3), RGS (regulators of G protein signaling), or RA domain, all of which may regulate protein localization. Based on the variety of domains in the SNX family, some authors speculate that only those SNXs containing a BAR domain would act as a "real" SNX, whereas the family members with protein-protein interaction domains might function as signaling molecules (31). According to this classification, SNX27 would belong to the latter group as it lacks the BAR domain but has a PDZ and an RA domain. SNX27 could thus act as a signaling platform, bringing proteins to vesicular compartments through PDZ-mediated interaction. Recent experiments identified SNX27 as responsible for the specific recruitment of the 5-hydroxytryptamine (4a) receptor to early endosomes, modulating the signaling pathway triggered by this receptor (34). The association of SNX27 with DGKζ described here points to a similar scenario in which SNX27 localization at 3-phosphorylated PI-enriched membranes would bring DGKζ into these compartments to exert its function. DGKζ localization to these structures would in turn contribute to stabilization of SNX27 in vesicles. Concurring with this hypothesis, we showed that disruption of the SNX27-DGKζ interaction by overexpression of a DGKζ C-terminal region results in a loss of vesicle localization similar to that observed for the SNX27 lacking the PDZ domain.

The SNX27·DGKζ complex would provide a mechanism for

[2] E. Rincón, T. Santos, A. Ávila-Flores, J. P. Albar, V. Lalioti, C. Lei, W. Hong, and I. Mérida, unpublished results.

regulating membrane DAG and PA levels in the ERC compartment. Accordingly we showed that DGKζ-knocked down cells have enhanced TfR recycling to the membrane, suggesting that DGKζ modulates the endocytic recycling pathway. Although their precise contribution to recycling kinetics remains to be fully elucidated, DAG and PA have well recognized membrane trafficking functions (2, 3, 9). Recent experiments showed that depletion of PLD_2, but not of PLD_1, inhibit the TfR recycling rate without affecting the internalization rate. HeLa cells with reduced PLD_2 show TfR accumulation in a Rab11-positive compartment, suggesting a role for PLD_2 in the endocytic recycling to the plasma membrane (41). Independent observations indicate that Arf6-mediated PLD activation is required for TfR and major histocompatibility complex protein class I recycling. Cells overexpressing Arf6 mutants defective in PLD activation inhibit major histocompatibility complex protein class I recycling to the plasma membrane; in these cells, propranolol treatment to increase PA levels by inhibiting phosphatidic acid phosphohydrolase does not rescue recycling, suggesting a requirement for phosphatidic acid phosphohydrolase-derived DAG rather than PA in this process (14). This is consistent with our results using DGKζ-depleted cells in which acceleration of TfR recycling might be due to DAG level increase and/or PA depletion.

In addition to its functions in membrane dynamics, DGKζ modulation of DAG levels may have other roles, such as decreasing protein activation/localization in the recycling endosome. Classical PKCs, such as PKCα and PKCβII, move to the ERC following their activation; this translocation has functional consequences because PKC regulates the dynamics of endocytosis and transferrin trafficking through the endocytic recycling pathway (61, 62). DGKζ is both a substrate and a potent modulator of PKCα; in this setting, SNX27-mediated DGKζ localization to the endosomal system would provide an additional mechanism for modulating PKC-regulated delivery of molecules to and from the ERC.

The endosomal system acts as an intracellular sorting network with a key role in decisions on the fate of internalized cargo. From the plasma membrane, internalized proteins reach the sorting endosomes where trafficking decisions are taken. Nutrient receptors such as TfR release their ligands and return to the plasma membrane. Signaling receptors can be recycled to the plasma membrane or progress to lysosomes where they are degraded (63). Sorting and recycling endosomes not only regulate traffic to and from the cell surface but also represent a major center for receiving and delivering biosynthetic traffic from the Golgi (31). Within the endosomal system, the ERC has an important function in polarized sorting of the endocytic and secretory pathways, promoting release of inflammatory cytokines to newly forming phagocytic cups in macrophages (64) or exocytosis of E-cadherin in epithelial cells (65). Here we characterized SNX27 as a component of the T lymphocyte endocytic recycling system and identified it as a DGKζ-interacting protein; this led to detection of a role for this enzyme in the regulation of exit traffic from the ERC. ERC-regulated recycling is necessary for efficient T cell receptor accumulation in the immunological synapse (IS). This recycling coincides with the TfR recycling pathway, and its inhibition leads to a reduction in TCR in the IS with a concomitant reduction in signaling (66, 67). T lymphocytes from DGKζ-deficient mice are hyperresponsive to *ex vivo* TCR stimulation and produce elevated cytokine levels in response to viral infection (24). Based on this observation and on our findings, we thus speculate that the absence of DGKζ in these mice contributes to the increase in TCR levels in the IS, enhancing the response.

The importance of endosomal trafficking regulation in T lymphocytes is highlighted by recent findings on the physiology of HIV-1-infected cells. Viral infection often profoundly modifies normal cell function to optimize viral propagation and cell survival. The HIV-1 Nef protein induces a severe reduction in TCR and Lck expression at the immunological synapse by inhibiting endocytosis and recycling (67). The identification of SNX27 as a DGKζ partner allows us to postulate new functions for this lipid kinase family in regulating the many functions ascribed to the endocytic recycling pathway.

Acknowledgments—We are grateful to colleagues who generously provided reagents. We thank Dr. I. Sandoval and I. Mérida group members for stimulating discussion, especially S. Carrasco for unconditional support to this work and critical assessment of the manuscript; S. Juarez for proteomics studies; A. Checa for confocal assistance; and C. Mark for excellent editorial assistance.

* This work was supported in part by Grants G03/79 from the Instituto de Salud Carlos III (Spanish Ministry of Health) and BFU2004-01756 (Spanish Ministry of Education) (to I. M.). The Department of Immunology and Oncology was founded and supported by the Spanish National Research Council (CSIC) and Pfizer. The costs of publication of this article were defrayed in part by the payment of page charges. This article must therefore be hereby marked "*advertisement*" in accordance with 18 U.S.C. Section 1734 solely to indicate this fact.

§ Recipient of Spanish Ministry of Education Fellowship AP2005-0189.

‖ Supported by the Juan de la Cierva program of the Spanish Ministry of Science and Technology.

¶¶ To whom correspondence should be addressed: Dept. of Immunology and Oncology, Centro Nacional de Biotecnología/CSIC, Darwin, 3, UAM Campus de Cantoblanco, E-28049 Madrid, Spain. Tel.: 34-915854702; Fax: 34-913720493; E-mail: imerida@cnb.uam.es.

REFERENCES

1. Gruenberg, J. (2003) Lipids in endocytic membrane transport and sorting. *Curr. Opin. Cell Biol.* **15,** 382–388
2. Goni, F. M., and Alonso, A. (1999) Structure and functional properties of diacylglycerols in membranes. *Prog. Lipid Res.* **38,** 1–48
3. Burger, K. N. (2000) Greasing membrane fusion and fission machineries. *Traffic* **1,** 605–613
4. Lentz, B. R., Malinin, V., Haque, M. E., and Evans, K. (2000) Protein machines and lipid assemblies: current views of cell membrane fusion. *Curr. Opin. Struct. Biol.* **10,** 607-s615
5. Jun, Y., Fratti, R., and Wickner, W. (2004) Diacylglycerol and its formation by phospholipase C regulate Rab- and SNARE-dependent yeast vacuole

fusion. *J. Biol. Chem.* **279,** 53186–53195
6. Baron, C., and Malhotra, V. (2002) Role of diacylglycerol in PKD recruitment to the TGN and protein transport to the plasma membrane. *Science* **295,** 325–328
7. Wong, T., Fairn, G., Poon, P., Shmulevitz, M., McMaster, C., Singer, R., and Johnston, G. (2005) Membrane metabolism mediated by Sec14 family members influences Arf GTPase activating protein activity for transport from the trans-Golgi. *Proc. Natl. Acad. Sci. U. S. A.* **102,** 12777–12782
8. Huttner, W. B., and Zimmerberg, J. (2001) Implications of lipid microdomains for membrane curvature, budding and fission. *Curr. Opin. Cell Biol.* **13,** 478–484
9. Kooijman, E., Chupin, V., de Kruijff, B., and Burger, K. (2003) Modulation of membrane curvature by phosphatidic acid and lysophosphatidic acid. *Traffic* **4,** 162–174
10. Kooijman, E. E., Chupin, V., Fuller, N. L., Kozlov, M. M., de Kruijff, B., Burger, K. N., and Rand, P. R. (2005) Spontaneous curvature of phosphatidic acid and lysophosphatidic acid. *Biochemistry* **44,** 2097–2102
11. Jenkins, G., Fisette, P., Anderson, R., and (1994) Type I phosphatidylinositol 4-phosphate 5-kinase isoforms are specifically stimulated by phosphatidic acid. *J. Biol. Chem.* **269,** 11547–11554
12. Jones, D. R., Sanjuan, M. A., and Merida, I. (2000) Type Iα phosphatidylinositol 4-phosphate 5-kinase is a putative target for increased intracellular phosphatidic acid. *FEBS Lett.* **476,** 160–165
13. Manifava, M., Thuring, J. W., Lim, Z. Y., Packman, L., Holmes, A. B., and Ktistakis, N. T. (2001) Differential binding of traffic-related proteins to phosphatidic acid- or phosphatidylinositol (4,5)-bisphosphate-coupled affinity reagents. *J. Biol. Chem.* **276,** 8987–8994
14. Jovanovic, O., Brown, F., and Donaldson, J. (2006) An effector domain mutant of Arf6 implicates phospholipase D in endosomal membrane recycling. *Mol. Biol. Cell* **17,** 327–355
15. Jackson, T. R., Brown, F. D., Nie, Z., Miura, K., Foroni, L., Sun, J., Hsu, V. W., Donaldson, J. G., and Randazzo, P. A. (2000) ACAPs are arf6 GTPase-activating proteins that function in the cell periphery. *J. Cell Biol.* **151,** 627–638
16. Luo, B., Regier, D. S., Prescott, S. M., and Topham, M. K. (2004) Diacylglycerol kinases. *Cell. Signal.* **16,** 983–989
17. Kanoh, H., Yamada, K., and Sakane, F. (2002) Diacylglycerol kinases: emerging downstream regulators in cell signaling systems. *J. Biochem.* (*Tokyo*) **131,** 629–633
18. Bunting, M., Tang, W., Zimmerman, G. A., McIntyre, T. M., and Prescott, S. M. (1996) Molecular cloning and characterization of a novel human diacylglycerol kinase ζ. *J. Biol. Chem.* **271,** 10230–10236
19. Sheng, M., and Sala, C. (2001) PDZ domains and the organization of supramolecular complexes. *Annu. Rev. Neurosci.* **24,** 1–29
20. Avila-Flores, A., Santos, T., Rincon, E., and Merida, I. (2005) Modulation of the mammalian target of rapamycin pathway by diacylglycerol kinase-produced phosphatidic acid. *J. Biol. Chem.* **280,** 10091–10099
21. Olenchock, B. A., Guo, R., Silverman, M. A., Wu, J. N., Carpenter, J. H., Koretzky, G. A., and Zhong, X. P. (2006) Impaired degranulation but enhanced cytokine production after FcεRI stimulation of diacylglycerol kinase ζ-deficient mast cells. *J. Exp. Med.* **203,** 1471–1480
22. Topham, M. K., Bunting, M., Zimmerman, G. A., McIntyre, T. M., Blackshear, P. J., Prescott, S. M. (1998) Protein Kinase C regulates the nuclear localization of DGKζ. *Nature* **394,** 697–700
23. Yakubchyk, Y., Abramovici, H., Maillet, J. C., Daher, E., Obagi, C., Parks, R. J., Topham, M. K., and Gee, S. H. (2005) Regulation of neurite outgrowth in N1E-115 cells through PDZ-mediated recruitment of diacylglycerol kinase ζ. *Mol. Cell. Biol.* **25,** 7289–7302
24. Zhong, X., Hainey, E. A., Olenchock, B. A., Jordan, M. S., Maltzman, J. S., Nichols, K. E., Shen, H., and Koretzky, G. A. (2003) Enhanced T cell responses due to diacylglycerol kinase ζ deficiency. *Nat. Immunol.* **4,** 882–890
25. Santos, T., Carrasco, S., Jones, D. R., Merida, I., and Eguinoa, A. (2002) Dynamics of diacylglycerol kinase ζ translocation in living T-cells. Study of the structural domain requirements for translocation and activity. *J. Biol. Chem.* **277,** 30300–30309
26. Hogan, A., Shepherd, L., Chabot, J., Quenneville, S., Prescott, S. M., Topham, M. K., and Gee, S. H. (2001) Interaction of γ1-syntrophin with diacylglycerol kinase-ζ. Regulation of nuclear localization by PDZ interactions. *J. Biol. Chem.* **276,** 26526–26533
27. Liu, Z., Chang, G. Q., and Leibowitz, S. F. (2001) Diacylglycerol kinase ζ in hypothalamus interacts with long form leptin receptor. Relation to dietary fat and body weight regulation. *J. Biol. Chem.* **276,** 5900–5907
28. Luo, B., Prescott, S., and Topham, M. (2003) Association of diacylglycerol kinase ζ with protein kinase C α: spatial regulation of diacylglycerol signaling. *J. Cell Biol.* **160,** 929–937
29. Davidson, L., Pawson, A. J., De Maturana, R. L., Freestone, S. H., Barran, P., Millar, R. P., and Maudsley, S. (2004) Gonadotropin-releasing hormone-induced activation of diacylglycerol kinase-ζ and its association with active c-src. *J. Biol. Chem.* **279,** 11906–11916
30. Worby, C. A., and Dixon, J. E. (2002) Sorting out the cellular functions of sorting nexins. *Nat. Rev. Mol. Cell. Biol.* **3,** 919–931
31. Carlton, J., Bujny, M., Rutherford, A., and Cullen, P. (2005) Sorting nexins—unifying trends and perspectives. *Traffic* **6,** 75–82
32. Hozumi, Y., Ito, T., Nakano, T., Nakagawa, T., Aoyagi, M., Kondo, H., and Goto, K. (2003) Nuclear localization of diacylglycerol kinase ζ in neurons. *Eur. J. Neurosci.* **18,** 1448–1457
33. Abramovici, H., Hogan, A., Obagi, C., Topham, M., and Gee, S. (2003) Diacylglycerol kinase-ζ localization in skeletal muscle is regulated by phosphorylation and interaction with syntrophins. *Mol. Biol. Cell* **14,** 4499–4511
34. Joubert, L., Hanson, B., Barthet, G., Sebben, M., Claeysen, S., Hong, W., Marin, P., Dumuis, A., and Bockaert, J. (2004) New sorting nexin (SNX27) and NHERF specifically interact with the 5-HT4a receptor splice variant: roles in receptor targeting. *J. Cell Sci.* **117,** 5367–5379
35. Seet, L. F., and Hong, W. (2001) Endofin, an endosomal FYVE domain protein. *J. Biol. Chem.* **276,** 42445–42454
36. Laemmli, U. K. (1970) Cleavage of structural proteins during the assembly of the head of bacteriophage T4. *Nature* **227,** 680–685
37. Shevchenko, A., Wilm, M., Vorm, O., and Mann, M. (1996) Mass spectrometric sequencing of proteins silver-stained polyacrylamide gels. *Anal. Chem.* **68,** 850–858
38. Palacios, S., Lalioti, V., Martinez-Arca, S., Chattopadhyay, S., and Sandoval, I. V. (2001) Recycling of the insulin-sensitive glucose transporter GLUT4. Access of surface internalized GLUT4 molecules to the perinuclear storage compartment is mediated by the Phe5-Gln6-Gln7-Ile8 motif. *J. Biol. Chem.* **276,** 3371–3383
39. Dai, J., Li, J., Bos, E., Porcionatto, M., Premont, R. T., Bourgoin, S., Peters, P. J., and Hsu, V. W. (2004) ACAP1 promotes endocytic recycling by recognizing recycling sorting signals. *Dev. Cell.* **7,** 771–776
40. Madrid, R., Janvier, K., Hitchin, D., Day, J., Coleman, S., Noviello, C., Bouchet, J., Benmerah, A., Guatelli, J., and Benichou, S. (2005) Nef-induced alteration of the early/recycling endosomal compartment correlates with enhancement of HIV-1 infectivity. *J. Biol. Chem.* **280,** 5032–5044
41. Padron, D., Tall, R. D., and Roth, M. G. (2006) Phospholipase D2 is required for efficient endocytic recycling of transferrin receptors. *Mol. Biol. Cell.* **17,** 598–606
42. Kajii, Y., Muraoka, S., Hiraoka, S., Fujiyama, K., Umino, A., and Nishikaws, T. (2003) A developmentally regulated and psychostimulant-inducible novel rat gene mrt1 encoding PDZ-PX protein isolated in the neocortex. *Mol. Psychiatry* **8,** 434–444
43. Cheever, M., Sato, T., de Beer, T., Kutateladze, T., Emr, S., and Overduin, M. (2001) Phox domain interaction with PtdIns(3)P targets the Vam7 t-SNARE to vacuole membranes. *Nat. Cell Biol.* **3,** 613–618
44. Ellson, C., Gobert-Gosse, S., Anderson, K., Davidson, K., Erdjument-Bromage, H., Tempst, P., Thuring, J., Cooper, M., Lim, Z., Holmes, A., Gaffney, P., Coadwell, J., Chilvers, E., Hawkins, P., and Stephens, L. (2001) PtdIns(3)P regulates the neutrophil oxidase complex by binding to the PX domain of p40(phox). *Nat. Cell Biol.* **3,** 679–682
45. Kanai, F., Liu, H., Field, S., Akbary, H., Matsuo, T., Brown, G., Cantley, L., and Yaffe, M. (2001) The PX domains of p47phox and p40phox bind to lipid products of PI(3)K. *Nat. Cell Biol.* **3,** 673–678
46. Xu, Y., Hortsman, H., Seet, L., Wong, S. H., and Hong, W. (2001) SNX3 regulates endosomal function through its PX-domain-mediated interaction with PtdIns(3)P. *Nat. Cell Biol.* **3,** 658–667
47. Ponting, C. P. (1996) Novel domains in NADPH oxidase subunits, sorting nexins, and PtdIns 3-kinases: binding partners of SH3 domains? *Protein Sci.* **5,** 2353–2357
48. Chen, J. W., Cha, Y., Yuksel, K. U., Gracy, R. W., and August, J. T. (1988) Isolation and sequencing of a cDNA clone encoding lysosomal membrane glycoprotein mouse LAMP-1. Sequence similarity to proteins bear-

ing onco-differentiation antigens. *J. Biol. Chem.* **263,** 8754–8758
49. Metzelaar, M. J., Wijngaard, P. L., Peters, P. J., Sixma, J. J., Nieuwenhuis, H. K., and Clevers, H. C. (1991) CD63 antigen. A novel lysosomal membrane glycoprotein, cloned by a screening procedure for intracellular antigens in eukaryotic cells. *J. Biol. Chem.* **266,** 3239–3245
50. Nakamura, N., Rabouille, C., Watson, R., Nilsson, T., Hui, N., Slusarewicz, P., Kreis, T. E., and Warren, G. (1995) Characterization of a cis-Golgi matrix protein, GM130. *J. Cell Biol.* **131,** 1715–1726
51. Mu, F. T., Callaghan, J. M., Steele-Mortimer, O., Stenmark, H., Parton, R. G., Campbell, P. L., McCluskey, J., Yeo, J. P., Tock, E. P., and Toh, B. H. (1995) EEA1, an early endosome-associated protein. EEA1 is a conserved α-helical peripheral membrane protein flanked by cysteine "fingers" and contains a calmodulin-binding IQ motif. *J. Biol. Chem.* **270,** 13503–13511
52. Gullapalli, A., Garrett, T. A., Paing, M. M., Griffin, C. T., Yang, Y., and Trejo, J. (2004) A role for sorting nexin 2 in epidermal growth factor receptor down-regulation: evidence for distinct functions of sorting nexin 1 and 2 in protein trafficking. *Mol. Biol. Cell* **15,** 2143–2155
53. Maxfield, F., and McGraw, T. (2005) Endocytic recycling. *Nat. Rev. Mol. Cell. Biol.* **5,** 121–132
54. Hazeki, O. (1995) Wortmannin, an inhibitor of phosphatidylinositol 3-kinase. *Seikagaku* **67,** 33–36
55. Ullrich, O., Reinsch, S., Urbe, S., Zerial, M., and Parton, R. G. (1996) Rab11 regulates recycling through the pericentriolar recycling endosome. *J. Cell Biol.* **135,** 913–924
56. Ren, M., Xu, G., Zeng, J., De Lemos-Chiarandini, C., Adesnik, M., and Sabatini, D. D. (1998) Hydrolysis of GTP on rab11 is required for the direct delivery of transferrin from the pericentriolar recycling compartment to the cell surface but not from sorting endosomes. *Proc. Natl. Acad. Sci. U. S. A.* **95,** 6187–6192
57. Zhong, X. P., Hainey, E. A., Olenchock, B. A., Zhao, H., Topham, M. K., and Koretzky, G. A. (2002) Regulation of T cell receptor-induced activation of the Ras-ERK pathway by diacylglycerol kinase ζ. *J. Biol. Chem.* **277,** 31089–31098
58. Fabre, S., Reynaud, C., and Jalinot, P. (2000) Identification of functional PDZ domain binding sites in several human proteins. *Mol. Biol. Rep.* **27,** 217–224
59. Carlton, J., Bujny, M., Peter, B., Oorschot, V., Rutherford, A., Mellor, H., Klumpermar, J., McMahon, H., and Cullen, P. (2004) Sorting nexin-1 mediates tubular endosome to TGN transport through the co-incidence sensing of high curvature membrane and 3-phosphoinositides. *Curr. Biol.* **14,** 1791–1800
60. Peter, B., Kent, H., Mills, IG, Vallis, Y., Butler, P., Evans, P., and McMahon, H. (2004) BAR domains as sensors of membrane curvature: the amphiphysin BAR structure. *Science* **303,** 495–499
61. Becker, K., and Hannun, Y. (2003) cPKC-dependent sequestration of membrane-recycling components in a subset of recycling endosomes. *J. Biol. Chem.* **278,** 52747–52754
62. Idkowiak-Baldys, J., Becker, K. P., Kitatani, K., and Hannun, Y. A. (2006) Dynamic sequestration of the recycling compartment by cPKC. *J. Biol. Chem.* **281,** 22321–22331
63. Sorkin, A., and Von Zastrow, M. (2002) Signal transduction and endocytosis: close encounters of many kinds. *Nat. Rev. Mol. Cell. Biol.* **3,** 600–614
64. Murray, R., Kay, J., Sangermani, D. G., and Stow, J. L. (2005) A role for the phagosome in cytokine secretion. *Science* **310,** 492–495
65. Lock, J., and Stow, J. (2005) Rab11 in recycling endosomes regulates the sorting and basolateral transport of E-cadherin. *Mol. Biol. Cell* **16,** 1744–1755
66. Das, V., Nal, B., Dujeancourt, A., Thoulouze, M. I., Galli, T., Roux, P., Dautry-Varsat, A., and Alcover, A. (2004) Activation-induced polarized recycling targets T cell antigen receptors to the immunological synapse; involvement of SNARE complexes. *Immunity* **20,** 577–588
67. Thoulouze, M. I., Sol-Foulon, N., Blanchet, F., Dautry-Varsat, A., Schwartz, O., and Alcover, A. (2006) Human immunodeficiency virus type-1 infection impairs the formation of the immunological synapse. *Immunity* **24,** 547–561